SYNTHESIS OF ZEOLITE-ACTIVATED CARBON COMPOSITE FOR REMOVAL OF AMMONIUM FROM AQUEOUS SOLUTION

Pham Thi Yen[1], Nguyen Thanh Dong[1], Nguyen Viet Hoang[1], Pham Tuan Linh[1], Nguyen Tien Vinh[2], Nguyen Thi Thu Trang[1, *]

[1]Institute of Environmental Technology, Vietnam Academy of Science & Technology, 18 Hoang Quoc Viet, Cau Giay, Ha Noi, Viet Nam

[2]University of Technology Sydney, PO Box 123, Broadway NSW 2007, Australia

[*]Email: thutrangnguyen1210@gmail.com

Abstract. In this study, zeolite-activated carbon composite (Z/AC) was synthesized by hydrothermal reaction using kaolin as a source of silica and alumina. The synthesized materials were characterized by Brunner-Emmet-Teller (BET) surface area to calculate surface area, X-ray diffraction (XRD) to study the crystal structure of materials, Infrared spectroscopy (IR) to indicate the presence of functional groups on the surface and scanning electron microscopy (SEM) to determine the morphology of the composites. In this paper, adsorption equilibrium and kinetics for the removal of ammonium by prepared Z/AC materials were evaluated.

1. INTRODUCTION

Over the past decade, a variety of biological, chemical, physical methods, or a combination of these methods have been studied to remove ammonium. Some traditional methods to remove ammonium in water such as the stripping process [1], reverse osmosis [2], nitrification - reduction, biological methods [3], chemical precipitation [4], and electrochemical [5] have been developed. However, there are some drawbacks to these technologies such as high cost, low removal rate, and low efficiency. Compared with other techniques, ion exchange and adsorption techniques have many advantages and convenience such as relatively high removal efficiency, varios materials, easily finding or synthesis, low price, high capacity and adsorption rate, convenient application in practice, as well as no difficulty in reconstitution and friendliness environment [6]. Therefore, the development of adsorbents and the improvement of water treatment processes to remove pollutants more effectively are important in environmental treatment.

Zeolite is a porous structure material containing many metal cations. The unique structure of zeolite enables it to exchange ions with an external medium. The ion exchange process takes place in the zeolite and can remove the ionized ammonium from water by exchanging it for another chemical ion in the exchange medium. Studies of Millar *et al.* [7] and Mazloomi *et al.*

[8] have shown that natural zeolites are capable of removing ammonium from water. Although natural zeolites are widely available, they are rarely used to remove ammonium in water due to its low adsorption capacity and low ammonium removal efficiency. Nowadays, many types of synthetic zeolite have been studied for ammonium removal in water. However, the disadvantage of using zeolite as an ion exchange is that this process is affected by other metal ions because ion exchange has a selective affinity for some metals such as Cs^+, K^+, Na^+, Mg^{2+}, Ca^{2+}, etc. So, it is necessary to promote the ammonium removal efficiency of zeolite through additional adsorbents or filtration processes to reduce the effects of metals and organic substances in the water [9]. Activated carbon (AC) with a high specific surface area, abundant pore volume, and functional groups including oxygen, hydrogen, sulfur, and nitrogen allows to adsorb organic compounds such as carboxyl, carbonyl, phenol, lactone, and quinone. Activated carbon works effectively in removing odors, discoloration as well as removing toxic organic substances, such as phosphates and lead [10].

Theoretically, the combination of activated carbon and zeolite will facilitate changes in chemical structure, physics, chemical bonding, and energy range distance in the zeolite, improve the ability to link intermolecular and enhance the stability and durability of materials. Moreover, the activated carbon material combined with zeolite can have the properties of both activated carbon and zeolite, forming new capillaries to create favorable conditions to improve the decomposition rate and ion exchange capacity of materials [5].

The purpose of this study is to determine the optimal conditions for the synthesis of zeolite and activated carbon (Z/AC) materials with silicate and aluminum from kaolin to obtain the best results for NH_4^+ adsorption. Synthesis parameters such as kaolin/activated carbon ratio and concentration of sodium hydroxide were studied and optimized to achieve materials that have a high ammonium removal efficiency. Besides, the effects of pH, stirring time, initial concentration on NH_4^+ adsorption capacities were investigated and clarified.

2. MATERIALS AND RESEARCH METHODS

2.1. Preparation of materials

Kaolin was taken from Phu Tho kaolin factory (Phu Tho, Viet Nam). The chemical reagents, such as sodium hydroxide (NaOH ≥ 97 %) and ammonium chloride (NH_4Cl ≥ 99.8 %) were purchased from Merck (Germany) and hydrochloric acid (HCl 37 % - 38 %) was purchased from Sigma-Aldrich (USA). Activated carbon powder was purchased from Tra Bac Joint stock company (Viet Nam).

Activating kaolin: Kaolin (66.28 % SiO_2, 20.28 Al_2O_3, 0.7 % total Fe) was pretreated and eliminated off large-sized mechanical impurities (gravel, quartz, etc.) by sieving through a sieve of different sizes 0.25 mm. To release small-sized mechanical impurities, kaolin was washed many times by deionized water. After being dried at 105^oC for 4 hours, kaolin was activated under the condition of 4N HCl acid solution, the ratio of kaolin/acid is 2/3 and stirring continuously for 6 hours. Then, the activated kaolin was washed and filtered with deionized water until the absence of Cl^- ion and dried at 105^oC for 4 hours.

2.2. Synthesis of Z/AC material

10 g of activated kaolin was mixed with an amount of NaOH for 30 min (the reaction takes place in a solid form), then heated at 600 °C for 1 hour. The calcinated product was ground and transferred completely to the Teflon flask. An appropriate amount of activated carbon and 100

76

ml of water were added and stirred at a speed of 500 rpm for 12 hours. Then, the mixture was aged at room temperature for 5 hours and crystallized at $100^{\circ}C$ for 12 hours. After that, the obtained solid was washed to neutral pH and dried at $100^{\circ}C$ [11].

2.3. Characterization of synthesized materials

The morphologies of the samples were observed by scanning electron microscopy (SEM). . The specific surface area of powder photocatalyst was measured using the Brunauer-Emmett-Teller method (BET) with a MicroActive TriStar II Plus 2.03 for N_2 BET at 77.35 K. The chemical bonds and functional groups of the material were assessed by Nexus 670 ThermoNicolet Fourier Transform infrared Spectrometer with a scan range of 4000–400 cm^{-1}. The phase compositions and crystal structures were examined by an X-ray diffractometer (XRD, D8 Advance – Bruker diffractometer) with Cu Kα radiation at the 2θ from 5° to 70°, in steps of $0.02^{o}/s$. The surface charge of the samples was examined using Zetasizer Nano Series (Malvern).

2.4. Adsorption experiments

The NH_4^+ adsorption capacity of synthesized materials was assessed by the absorption of ammonium from aqueous solutions. 0.1 g of Z/AC was added to a 100 ml volumetric flask of ammonium solution and stirred at room temperature and a constant rate. Initial NH_4^+ concentration of 25 mg/l was used to study the effect of pH, time, and the temperature on the adsorption capacity of the material. The pH of the solution was maintained constant during each adsorption test by adjusting with 0.1M NaOH or 0.1M HCl solution. The effect of the initial concentration was assessed with the initial NH_4^+ concentration of 10, 20, 40, 50, 60, 80, 100 mg/l. Each experiment was repeated 3 times for calculating the mean average concentration. NH_4^+ concentration was determined by a photometric method. The adsorption capacity (q_t) at time t was calculated by the formula: $q_t = (C_0-C_t) \times V/m$ and adsorption capacity in equilibrium: $q_e = (C_0-C_e) \times V/m$; where C_0 is initial NH_4^+ concentration, C_t and C_e are NH_4^+ concentrations at time t and equilibrium, V is the volume of NH_4^+ solution, m is the weight of adsorbent.

3. RESULTS AND DISCUSSION

3.1. Characteristics of materials

Figure 1 illustrated the XRD patterns of the Z/AC samples with different kaolin/AC ratio and concentration NaOH. When the concentration of NaOH increases, the characteristic diffuse peaks of kaolin gradually disappears, indicating that the structure of crystalline kaolins has changed. However, some strong and sharp diffraction peaks appear in the FAU zeolite, indicating the formation of a new crystalline substance. The characteristic peaks for FAU zeolite appeared at angles $2\theta = 6.1^{o}$; 15.5^{o}; 23.5^{o}; 31° which is consistent with the reference values for FAU zeolite [12, 13]. Thus, it was found that under the condition of hydrothermal crystallization, the shift has been transferred from an amorphous structure of kaolin to form zeolite crystals. Fig. 1b showed that when the kaolin/AC ratio increased continuously, the relative intensities of the XRD peaks of the synthetic material were found to increase because of the relative augment of the zeolite crystal phase in Z/AC composite.

Figure 2b shows the adsorption-desorption isotherm is assigned to the type IV isotherm with the H3 hysteresis loop [13]. The vertical coordinate values (relative intensity) of sample Z/AC (kaolin/AC = 4) are higher than those of Zeolite samples; it shows a steep increase in N_2 adsorption at the low-pressure region ($P/P_0 < 0.05$) and the number of micropores (< 2 nm)

increases when a small amount of activated carbon is present. The isotherm of sample Z/AC also had a hysteresis loop at the high-pressure region ($P/P_0 > 0.5$), evidencing the existence of pores. It was noted that the hysteresis loop has increased at about $P/P_0 > 0.9$, which means that the number of macropores rapidly increased as more activated carbon was added (Fig. 2b). BET specific surface area and total pore volume (Table 1) of Z/AC samples are 231.219 m²/g and 0.220 cm³/g, respectively. This result is 1.8 times higher than zeolite, demonstrating that the presence of activated carbon could greatly enhance the specific surface area and increase the diversity of the pore structure.
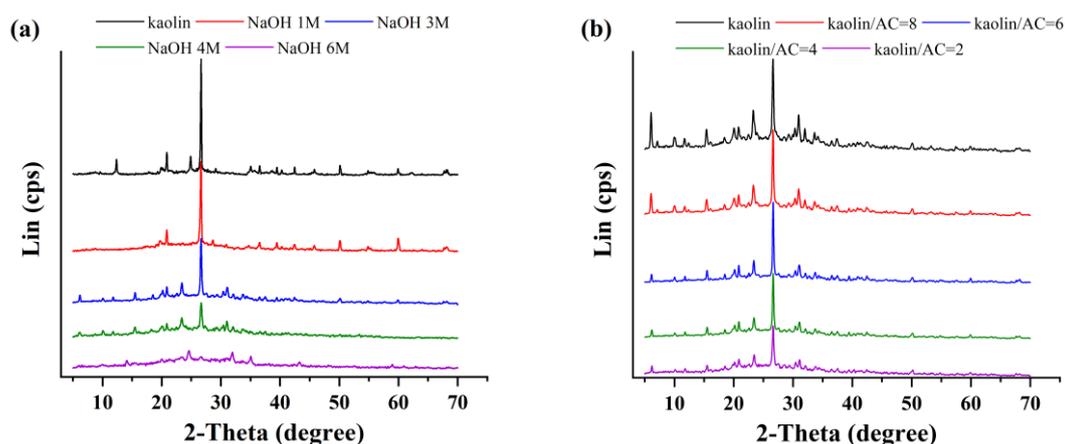

Figure 1. XRD patterns of the Z/AC samples with different concentration NaOH (Kaolin/AC = 4) (a) and kaolin/AC ratios (3M NaOH) (b).
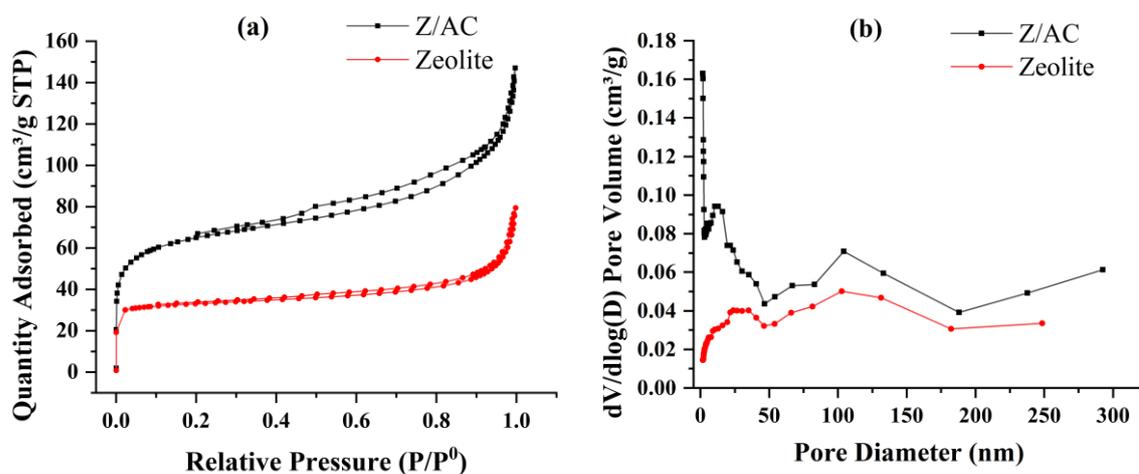

Figure 2. Nitrogen adsorption and desorption isotherms (a) and pore diameter distribution of the Z/AC (kaolin/AC = 4) and zeolite sample (b).

The zeta potential results of the Z/AC and zeolite samples are shown in Fig. 3, which indicates that the zeolite surface groups are mostly negatively charged within the studied pH range. Besides, the presence of activated carbon does not change the zeta potential of the prepared zeolite samples
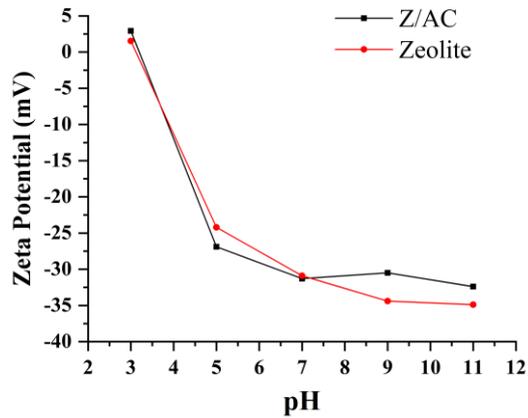
Figure 3. Variation of zeta potential versus pH for the Z/AC and zeolite samples.

Table 1. Morphology and pore structure of synthesized samples.

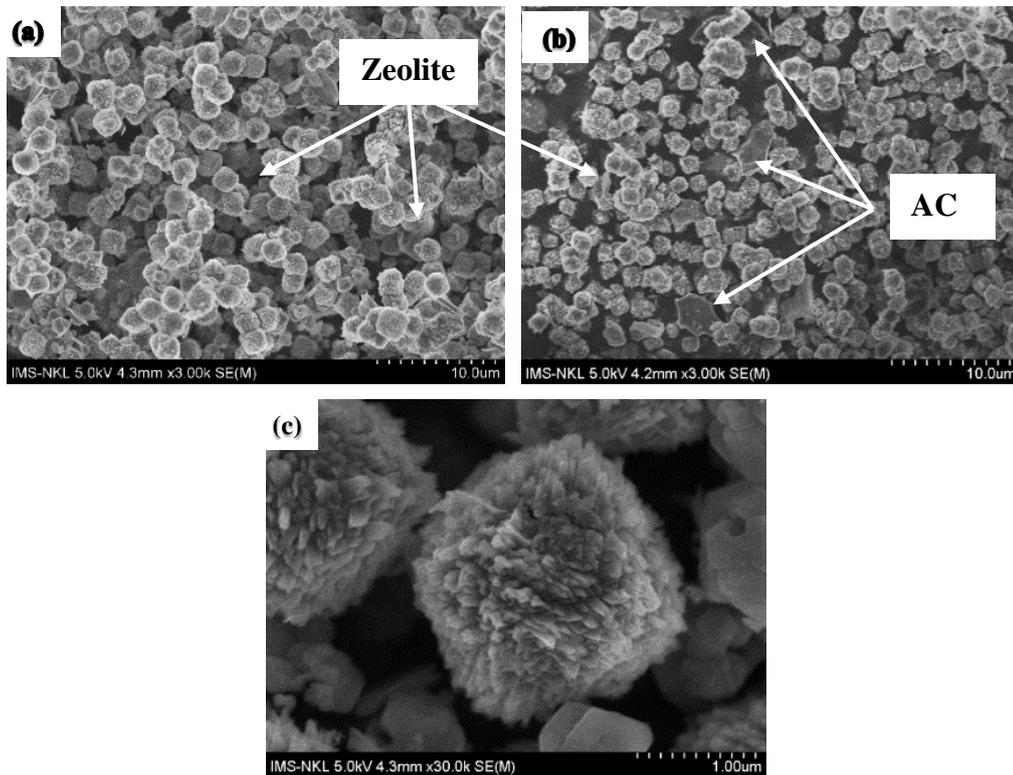| Samples	BET Surface Area (m²/g)	Total pore volume (cm³/g)	Average pore diameter (nm)
Z/AC	231.219	0.220	3.805
Zeolite	127.967	0.116	3.630

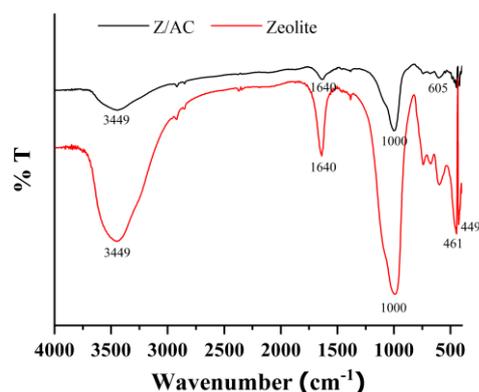*Figure 4.* SEM images of zeolites (a, c) and Z/AC (kaolin/AC =4) (b).

Figure 5. IR spectra of the Z/AC (kaolin/AC = 4) and zeolite samples.

SEM images of zeolite and Z/AC samples (Fig. 4) showed clearly that zeolite crystals had octahedral shape with fairly uniform size (about 2 μm) and good dispersion. SEM image of the Z/AC sample (Fig. 4b) presented the appearance of small activated carbon fragments with irregular shape, next to the zeolite crystals.

Figure 5 showed the IR spectrum of the zeolite sample in the range of 400-4000 cm^{-1}. The characteristic peaks of H_2O were observed at 1640 cm^{-1} and 3449 cm^{-1}; the characteristic peak at 1640 cm^{-1} was caused by the bending vibration of H-O-H in the adsorbed water and the characteristic peak at 3449 cm^{-1} was caused by the OH- hydrogen-bond stretching vibration. The strongest band near 1000 cm^{-1} was attributable to the (Si, Al)-O asymmetric stretching modes. The bands at 449 cm^{-1} and 461 cm^{-1} were attributable to the internal (Si, Al)- O_4 tetrahedral bending modes [13], [14]. The IR spectrum of the zeolite sample had a much greater vibration amplitude than the Z/AC sample due to the lower zeolite content in the Z/AC sample. Besides, in the IR spectrum of the Z/AC sample, peak 605 cm^{-1} was characteristic of the C-H bond in the Z/AC sample, indicating a change in Z/AC structure compared to zeolite [15].

3.2. Optimal conditions for synthesis Z/AC

Figure 6a showed the NH_4^+ adsorption capacity of Z/AC increased with the increasing of the kaolin/AC ratio to 4, the q_e value reached a maximum of 18.10 mg/g. Further increasing the ratio of kaolin/AC, the q_e value decreased to 9.19 mg/g with kaolin/ AC = 8. It was notable that the NH_4^+ adsorption capacity of pure kaolin was almost 1.84 mg/g, much lower than the NH_4^+ adsorption capacity of Z/AC, whereas that was 13.1 mg/g on kaolin after hydrothermal treatment (zeolite). Adding a small amount of AC increased the dispersion of zeolite, which promoted the contact between zeolite and NH_4^+, and then lead to improve NH_4^+ adsorption. Therefore, the kaolin/AC ratio of 4 was chosen to use in the following experiments.

As Figure 6b showed, the NH_4^+ adsorption capacity increased with the increase of the NaOH concentration, when the concentration of NaOH increased to 3M, the q_e value reached the maximum capacity, which was 18.10 mg/g. When the concentration of NaOH greater than 3M, q_e value decreased gradually to 10.47 mg/g with a 6M NaOH solution. Therefore, under the synthesis condition of the 3M NaOH solution, the NH_4^+ adsorption capacity was the most effective.
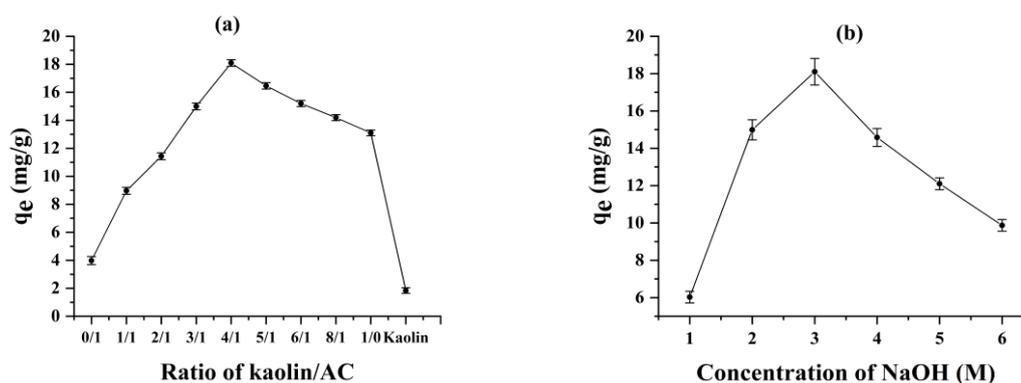
Figure 6. The effect of the ratio of kaolin/AC (a), the concentration of NaOH on the adsorption of NH_4^+ of the Z/AC samples (Condition: (a) $C_0 = 25$ mg/l, 3M NaOH; (b) $C_0 = 25$ mg/l, kaolin /AC = 4).

3.3. Survey of adsorption conditions

3.3.1. The effect of adsorption time

The adsorption capacity results (Fig. 7a) showed that the NH_4^+ adsorption capacity of Z/AC increased from 14.5 mg/g to 18.01 mg/g in 2 to 30 min. After about 30 to 150 min of adsorption, the adsorption capacity did not increase significantly, indicating that the material has reached the adsorption equilibrium and the absorption capacity of 18.10 mg/g. Therefore, the stirring time of 45 min was selected as the optimum stirring time on the NH_4^+ adsorption of the Z/AC sample.

3.3.2. The effect of pH

pH plays an important role in the adsorption processes because it influences the chemical balance between ammonium ions and ammonia, according to the following reversible reaction:

$$NH_3 + H_2O \leftrightarrow NH_4^+ + OH^-$$
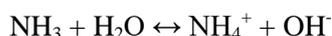
The effects of pH on ammonium adsorption capacity and removal efficiency of the synthesized material samples were evaluated in the range of pH from 3 to 10 to select the most suitable conditions for adsorption (Fig. 7b). The results showed that the maximum adsorption capacity of NH_4^+ was achieved at pH of 7. As mentioned in the results of the zeta potential measurement, the zeolite surface in the studied pH range always has a negative charge, which is favorable for the adsorption of positive charged ions. According to the relation of ammonia dissolution in water as a function of pH, the ammonium ion and ammonia are the dominant species in the water at pH below 7 and alkaline pH, respectively. When pH is lower than 7, ammonium ions compete with hydrogen ions on the adsorption sites of zeolite. Increasing the adsorption of ammonia when increasing the pH of the water to the maximum point (pH 7) could be due to a decrease in H ions in the solution, and thus reducing the competition of these H ions with ammonium ions on adsorption sites of zeolite molecules. When pH value is higher than 7, the adsorption capacities of NH_4^+ decrease because ammonium ion is transformed into nonionized forms of ammonia gas, which is a disadvantage for adsorption on zeolite Z/AC.

Therefore, in this study, the pH of 7 was selected as the optimum pH on the NH_4^+ the adsorption of the Z/AC sample. This work had similar results on ammonium adsorption onto zeolite utilization to the results of studies by other researchers [16, 17].

3.3.3. *The effect of initial NH$_4^+$ concentration*

Research results on the effect of the initial ammonium concentration on the adsorption capacity of the material are shown in Fig. 7c. When the initial ammonium concentration increased from 10 to 100 mg/l, the ammonium adsorption capacity also increased from 8.23 to 41.11 mg/g. The increase in initial NH$_4^+$ concentration would lead to a rise in mass transfer driving force and therefore the rate ammonium ions pass from the bulk solution to the particle surface. The equilibrium was achieved when all the exchangeable ammonium and cation on the external and internal surfaces of the zeolite were reached.
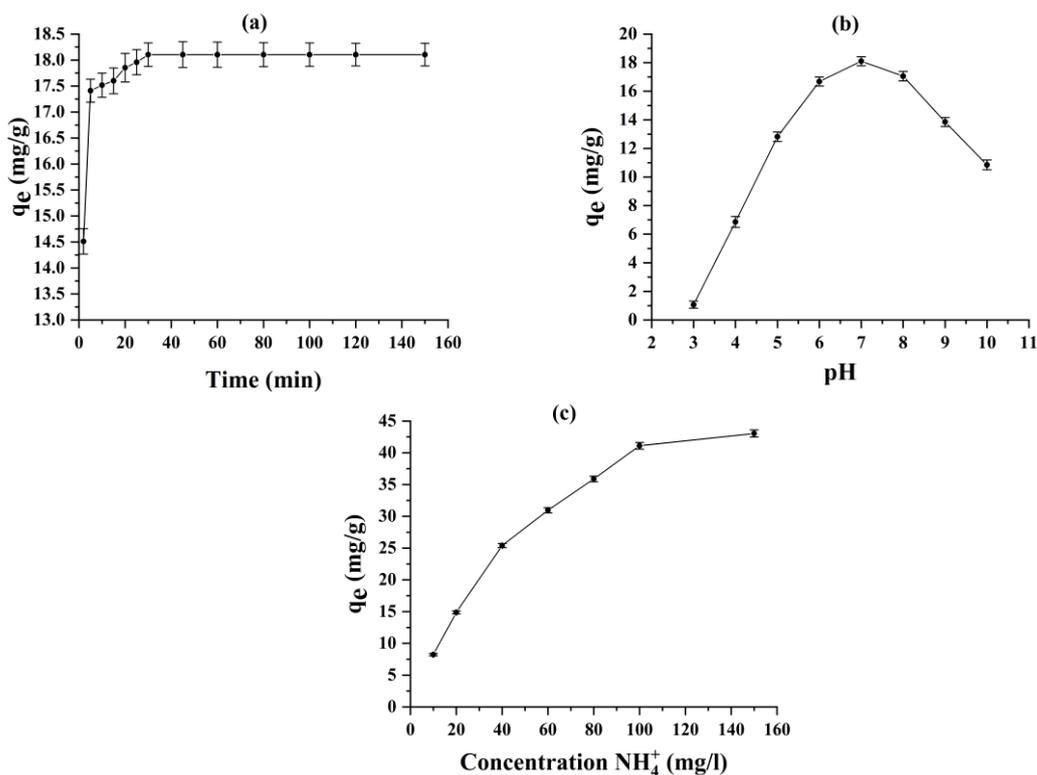

Figure 7. The effect of stirring time (a), pH (b), initial NH$_4^+$ concentration (c) on the adsorption of NH$_4^+$ of the Z/AC sample (Condition: (a) C$_0$ = 25 mg/l, pH = 7; (b) C$_0$ = 25 mg/l, stirring time 45 min; (c) pH = 7, stirring time 45 min).

4. CONCLUSION

In the study, the Z/AC composite was successfully synthesized for NH$_4^+$ removal from aqueous solution. Kaolin/AC ratio of 4 and 3M NaOH was chosen as the optimal condition to synthesize Z/AC materials. BET specific surface area and total pore volume of the Z/AC sample are 231.219 m²/g and 0.220 cm³/g, respectively. Even a negligible amount of AC is included, it could lead to a growth in specific surface areas BET and dispersion of Z/AC, which promoted the contact between zeolite and NH$_4^+$ and improved the NH$_4^+$ adsorption capacity. The maximum adsorption amount of NH$_4^+$ of this Z/AC material is 18.10 mg/g with an initial concentration of 25 mg/l, optimal adsorption condition of pH = 7, the stirring time of 45 min.

These results showed that Z/AC is a promising material in adsorption to remove NH_4^+ from aqueous solution.

REFERENCES

1. Guštin S. and Marinšek Logar R. - Effect of pH, temperature and air flow rate on the continuous ammonia stripping of the anaerobic digestion effluent, Process Safety and Environmental Protection. 89 (1) (2011) 61-66.
   https://doi.org/10.1016/j.psep.2010.11.001.

2. Cancino-Madariaga M., Hurtado F. C., and Ruby R. - Effect of pressure and pH in ammonium retention for nanofiltration and reverse osmosis membranes to be used in recirculation aquaculture systems (RAS), Aquacultural Engineering **45** (3) (2011) 103-108. https://doi.org/10.1016/j.aquaeng.2011.08.002.

3. Feng S., Xie S., Zhang X., and Yang Z. - Ammonium removal pathways and microbial community in GAC-sand dual media filter in drinking water treatment, Journal of Environmental Sciences (China) **24** (9) (2012) 1587-1593.
   https://doi.org/10.1016/j.jece.2015.11.031.

4. Huang J., Kankanamge N. R., Chow C., Welsh D. T., Li T., and Teasdale R. P. - Removing ammonium from water and wastewater using cost-effective adsorbents: A review, Journal of Environmental Sciences (China) **63** (2018) 174-197.
   https://doi.org/10.1016/j.jes.2017.09.009.

5. [5]   Foo Y. K. and Hameed H. B. - The environmental applications of activated carbon/zeolite composite materials, Advances in Colloid and Interface Science. 162 (1–2) (2011) 22–28. https://doi.org/10.1016/j.cis.2010.09.003.

6. Tahir E. and Everest E. - Low-Dimensional and Nanostructured Materials and Devices, Springer Champp, 2016. https://doi.org/10.1007/978-3-319-25340-4.

7. Millar G. J., Winnett A., Thompson T., and Couperthwaite S. J. - Equilibrium studies of ammonium exchange with Australian natural zeolites, Journal of Water Process Engineering **9** (2016) 47-57. https://doi.org/10.1016/j.jwpe.2015.11.008.

8. Mazloomi F. and Jalali M. - Ammonium removal from aqueous solutions by natural Iranian zeolite in the presence of organic acids, cations and anions, Journal of Environmental Chemical Engineering **4** (1) (2016) 240-249.
   https://doi.org/10.1016/j.jece.2015.11.031.

9. Liang L. Z., Chen H., Rong B. Z., and Zheng L. H. - Combination of powdered activated carbon and powdered zeolite for enhancing ammonium removal in micro-polluted raw water, Chemosphere **134** (2015) 127-132.
   https://doi.org/10.1016/j.chemosphere.2015.03.088.

10. Yua L. J., Rengasamya K., Limb K. Y., Tanc L. S., and Tarawnehd M. - Comparison of activated carbon and zeolites' filtering efficiency in freshwater, Journal of Environmental Chemical Engineering **7** (4) (2019). https://doi.org/10.1016/j.jece.2019.103223.

11. Robson H. - Verified Synthesis of Zeolitic Materials: Second Edition, Elsevier Science, 2001. https://doi.org/10.1016/B978-0-444-50703-7.X5094-7

12. Lia H., Zheng F., Wang J., Zhou J., Huang X., and Chen L. - Facile preparation of zeolite-activated carbon composite from coal gangue with enhanced adsorption performance, Chemical Engineering Journal **390** (2020). https://doi.org/10.1016/j.cej.2020.124513.

13. Yusof A. M., Nizam N. A., and Rashid N. A. - Hydrothermal conversion of rice husk ash to faujasite-types and NaA-type of zeolites, Journal of Porous Materials **17** (1) (2010) 39-47. https://doi.org/10.1007/s10934-009-9262-y.

14. Wang P., Sun Q., Zhang Y., and Cao J. - Effective removal of methane using nano-sized zeolite 4A synthesized from kaolin, Inorganic Chemistry Communications **111** (2020). https://doi.org/10.1016/j.inoche.2019.107639.

15. Wang M., Xie R., Chen Y., Pu X., Jiang W., and Yao L. - A novel mesoporous zeolite-activated carbon composite as an effective adsorbent for removal of ammonia-nitrogen and methylene blue from aqueous solution, Bioresource Technology **268** (2018) 726-732. https://doi.org/10.1016/j.biortech.2018.08.037.

16. Zhang Y., Yu F., Cheng W., Wang J., and Ma J. - Adsorption Equilibrium and Kinetics of the Removal of Ammoniacal Nitrogen by Zeolite X/Activated Carbon Composite Synthesized from Elutrilithe, Journal of Chemistry **9** (2017).

https://doi.org/10.1155/2017/1936829.

17. Alshameri A., Yan C., Al-Ani Y., Dawood A. S., and Ibrahim A. - An investigation into the adsorption removal of ammonium by salt activated Chinese (Hulaodu) natural zeolite: Kinetics, isotherms, and thermodynamics, Journal of the Taiwan Institute of Chemical Engineers **45** (2) (2014) 554-564. https://doi.org/10.1016/j.jtice.2013.05.008.